

# Effects of inter-nucleon correlations on the pion yields in heavy-ion collisions at medium energies

Zu-Xing Yang<sup>1,2,\*</sup>, Nicolas Michel<sup>1,†</sup>, Xiao-Hua Fan<sup>3</sup>, and Wei Zuo<sup>1,2</sup>

<sup>1</sup>*Institute of Modern Physics, Chinese Academy of Sciences, Lanzhou 730000, China*

<sup>2</sup>*School of Nuclear Science and Technology, University of Chinese Academy of Sciences, Beijing 100049, China*

<sup>3</sup>*School of Physical Science and Technology, Southwest University, Chongqing 400715, China*

We study a problem of pion production in heavy ion collision in the context of the Isospin-dependent Boltzmann-Uehling-Uhlenbeck transport model. In order to ponder the effect of inter-nucleon correlations on pion yields, we generated nucleon densities using two different models, the Skyrme-Hartree-Fock model and configuration interaction shell model. Indeed, inter-nucleon correlations are explicitly taken into account in shell model, while they are averaged in the Skyrme-Hartree-Fock model. As an application of our theoretical frameworks, we calculated the  $\pi^-$  and  $\pi^+$  yields in collisions of nuclei with  $A = 30 - 40$  nucleons. It is found that the amount of the produced  $\pi^-$  and  $\pi^+$  mesons is larger using the shell model framework, whereas the  $\pi^-/\pi^+$  ratios bear similar values in both used models. Our calculations suggest that further study should be made to determine whether the Skyrme-Hartree-Fock model or shell-model framework is more appropriate to reproduce experimental pion yields.

## I. INTRODUCTION

Research on heavy-ion collisions(HIC) has been extensively performed experimentally and theoretically over the past few decades [1]. While the theoretical description has relied on phenomenology for a long time [2], microscopic models have been developed in order to have a more realistic approach of HIC [1–3]. It has been shown recently that inclusion of pairing correlations can significantly modify reaction observables such as counts of emitted protons in proton-target reactions at intermediate energies by exploring the density profile of target nuclei[4]. Deformation and orientation effects have also been noticed to be important for particle production in uranium-uranium collisions at relativistic energies [5]. Consequently, both structure and reaction dynamics are important for the description of nucleus-nucleus collisions.

In order to calculate the pion yields produced during the collisions of medium and heavy nuclei, the Isospin-dependent Boltzmann-Uehling-Uhlenbeck (IBUU) transport model is often used. Recent experimental data consist of the  $^{197}\text{Au} + ^{197}\text{Au}$  reaction at 400 MeV/nucleon for incident energy within the ASY-EOS experiment at the GSI laboratory [6], and of the  $^{132}\text{Sn} + ^{132}\text{Sn}$  reaction at a beam energy of 0.3 GeV/nucleon, carried out at RIKEN in Japan [7]. They could provide information about the equation of state (EOS) [8–11], short-range correlations (SRC) [12] and medium effects in scattering cross sections [13, 14]. Both theoretical and experimental studies have pointed out that the  $\pi$  meson is one of the promising probes to study the nuclear structure and reaction aspects of heavy ion collisions [9, 10, 14, 15]. The importance of  $\pi$  mesons for constraining the EOS

of asymmetric nuclear matter was firstly pointed out by Bao-An Li et al [15]. In recent years, Stone et al have studied systematically the effects of the proton and neutron density distributions in central heavy-ion collisions, and found the maximum neutron-to-proton ratio during the collision process is quite sensitive to the initial-state density distributions[16]. In the case of incident energy near the  $\pi$  meson threshold, it happens that the  $\pi$  meson is essentially generated by the decay of the  $\Delta_{1232}$  resonant state, whereas the  $N^*$  resonant state can be ignored [1, 15]. It was also shown recently that  $\pi$  mesons provide a remarkably good probe to study bubble structure inside nuclei [17].

Since the original work of Skyrme in the 1950s[18] and the parameterization of the original interactions by Vautherin and Brink in the early 1970s [19], considerable efforts have been made to include effective density-dependent interactions at mean-field level to study the properties of finite nuclei and nuclear matter. In fact, the SHF model, used along with density functional theory, is one of the most efficient and widely used models to study the bulk properties of nuclei all over the nuclear chart [18, 20, 21].

The contribution of the wave function provided by the mean-field Slater determinant describing nuclear ground states does not exceed 70% typically, it is necessary to use models beyond mean-field to account more realistically for two-body interactions in nuclear wave functions [22]. In order to include the main effects of inter-nucleon correlations, while dealing with a numerically tractable model, we chose to use the core + valence nucleons shell model (SM) approach [22–25]. The aim of this article is then to accurately simulate experimental situations with the SHF and SM approaches, in order to identify the main effects of inter-nucleon correlations on pion yields. Indeed, the SHF and SM approaches are typically used to theoretically calculate different types of physical observables. Bulk properties of nuclei, such as binding and Coulomb energies, mass root-mean-square radii, neutron

\* yangzuxing16@impcas.ac.cn

† nicolas.michel@impcas.ac.cn

skins, are properly reproduced by SHF [26–28]. Using the modified Fermi distributions [29–31] or Fourier-Bessel expansions[29, 32], radial density distributions consistent with experimental data can also be obtained [33]. Conversely, nuclear energy spectra, electromagnetic transitions, quadrupole moments and photo-nuclear reaction cross sections, i.e. observables depending on the detailed structure wave function, can be obtained with SM clearly using a properly devised effective interaction[22]. However, no attempt has been made to apply the density distribution of nucleons using wave functions derived from SM to initialize transport model for HIC in the context of pion productions. Hence, in this work, both SHF and SM approaches will be used to evaluate nucleon densities, which are then adopted in the isospin dependent BUU model to calculate  $\pi^-$  and  $\pi^+$  meson yields in HIC. We will consider nuclei of  $sd$ -shell, bearing  $A = 30 - 40$  nucleons. Indeed, SHF can be reliably used in these nuclei due to their sizable number of nucleons, on the one hand, while SM leads to tractable shell model spaces in the considered region of nuclear chart, on the other hand. The Hamiltonians used consist of the SkM\* interaction in SHF, which is widely applied for finite nuclei and nuclear matter [4, 34], while the USDB interaction will be considered as SM interaction (which one will denote as USDB-SM), as it has proved to properly describe the properties of nuclei of  $sd$  shell [35]. However, as there are no experimental data available in this region of the nuclear chart, we will only compare the theoretical results obtained with SHF and SM approaches.

## II. THE IBUU TRANSPORT MODEL

The phase-space distribution function  $f(\vec{r}, \vec{p}, t)$  of nucleons is needed to calculation the pion yields in HIC. In the IBUU model[15] the time-evolution of  $f(\vec{r}, \vec{p}, t)$  is described by the following transport equations:

$$\frac{\partial f}{\partial t} + \nabla_{\vec{p}} E \cdot \nabla_{\vec{r}} f - \nabla_{\vec{r}} E \cdot \nabla_{\vec{p}} f = I_c, \quad (1)$$

where  $E$  is the single particle energy which contains the kinetic energy  $E_{kin}$  and potential energy  $U$ . The left and right sides of Eq.(1) represent the time evolution and collision item of a single particle in the mean field, respectively.

In this model, the single nucleon potential  $U$  is a function of nucleon densities and reads [14, 36]:

$$\begin{aligned} U(\rho, \delta, \vec{p}, \tau) = & A_u(x) \frac{\rho_{\tau'}}{\rho_0} + A_l(x) \frac{\rho_{\tau}}{\rho_0} \\ & + B \left( \frac{\rho}{\rho_0} \right)^{\sigma} (1 - x\delta^2) - 8x\tau \frac{B}{\sigma + 1} \frac{\rho^{\sigma-1}}{\rho_0^{\sigma}} \delta \rho_{\tau'} \\ & + \frac{2C_{\tau, \tau}}{\rho_0} \int d^3 p' \frac{f_{\tau}(\vec{r}, \vec{p}')} {1 + (\vec{p} - \vec{p}')^2 / \Lambda^2} \\ & + \frac{2C_{\tau, \tau'}}{\rho_0} \int d^3 p' \frac{f_{\tau'}(\vec{r}, \vec{p}')} {1 + (\vec{p} - \vec{p}')^2 / \Lambda^2}, \end{aligned} \quad (2)$$

where  $\tau, \tau' = 1/2(-1/2)$  is the isospin projection of neutrons (protons),  $\delta = (\rho_n - \rho_p)/(\rho_n + \rho_p)$  denotes the isospin asymmetry, and  $\rho_n, \rho_p$  denote neutron and proton number densities, respectively. The parameters  $A_u(x), A_l(x), B, C_{\tau, \tau}, C_{\tau, \tau'}, \sigma, \Lambda$  are standard in the IBUU model and their definition can be found in Ref.[36]. And  $x = 1$  for the soft symmetry energy parameter  $x$  is used in this work.

The following formula is used for the  $\Delta$  resonance potential:

$$\begin{aligned} U^{\Delta^-} &= U_n, & U^{\Delta^0} &= \frac{2}{3}U_n + \frac{1}{3}U_p, \\ U^{\Delta^+} &= \frac{1}{3}U_n + \frac{2}{3}U_p, & U^{\Delta^{++}} &= U_p. \end{aligned} \quad (3)$$

The effective masses of neutron, proton and  $\Delta$  resonance are directly deduced from their corresponding potential, i.e.,

$$\frac{m_B^*}{m_B} = 1 / \left( 1 + \frac{m_B}{p} \frac{dU}{dp} \right). \quad (4)$$

One obtains the isospin-dependent baryon-baryon (BB) scattering cross section in medium,  $\sigma_{BB}^{\text{medium}}$ :

$$\begin{aligned} R_{\text{medium}}^{BB}(\rho, \delta, \vec{p}) &\equiv \sigma_{BB_{\text{elastic, inelastic}}}^{\text{medium}} / \sigma_{BB_{\text{elastic, inelastic}}}^{\text{free}}, \\ &= (\mu_{BB}^* / \mu_{BB})^2 \end{aligned} \quad (5)$$

where  $\mu_{BB}$  and  $\mu_{BB}^*$  are the reduced masses of the colliding baryon pairs in free space and medium, respectively, and  $\sigma_{BB_{\text{elastic, inelastic}}}^{\text{free}}$  is the free BB scattering cross section. The elastic proton-proton cross section  $\sigma_{pp}$  and neutron-proton cross section  $\sigma_{np}$  are taken from experimental data, and  $\sigma_{nn}$  is assumed to be equal to  $\sigma_{pp}$ . The  $N\Delta$  free elastic cross sections are assumed to be equal to nucleon-nucleon (NN) elastic cross sections at the same center of mass energy. The inelastic NN cross sections read:

$$\begin{aligned} \sigma^{pp \rightarrow n\Delta^{++}} &= \sigma^{nn \rightarrow p\Delta^-} = \sigma_{10} + \frac{1}{2}\sigma_{11} \\ \sigma^{pp \rightarrow p\Delta^+} &= \sigma^{nn \rightarrow n\Delta^0} = \frac{3}{2}\sigma_{11} \\ \sigma^{np \rightarrow p\Delta^0} &= \sigma^{np \rightarrow n\Delta^+} = \frac{1}{2}\sigma_{11} + \frac{1}{4}\sigma_{10} \end{aligned} \quad , \quad (6)$$

and are parametrized via[1],

$$\sigma_{II'}(s) = \frac{\pi(\hbar c)^2}{2p^2} \alpha \left( \frac{p_r}{p_0} \right)^{\beta} \frac{m_0^2 \Gamma^2 (q/q_0)^3}{(s^* - m_0^2)^2 + m_0^2 \Gamma^2}, \quad (7)$$

where  $s^* = \langle M \rangle^2$ ,  $p_r^2(s) = \frac{[s - (m_N - \langle M \rangle)^2][s - (m_N + \langle M \rangle)^2]}{4s}$ ,  $q^2(s^*) = \frac{[s^* - (m_N - m_{\pi})^2][s^* - (m_N + m_{\pi})^2]}{4s^*}$ ,  $q_0 = q(m_0^2)$ , and  $I, I'$  represent the initial state and final state isospins of two nucleons. As for  $\alpha, \beta, m_0$ , and  $\Gamma$ , there are four parameter sets for  $\sigma_{10}^d, \sigma_{11}, \sigma_{10}, \sigma_{01}$ . Details concerning the value  $\langle M \rangle$  and the four  $\sigma$  parameter sets can be find in Ref. [37].

The mass of the produced  $\Delta$  baryons in Eqs.(5,6,7) is described by a modified Breit-Wigner function[38].

$$P(m_\Delta) = \frac{p_f m_\Delta \times 4m_{\Delta_0}^2 \Gamma_\Delta}{(m_\Delta^2 - m_{\Delta_0}^2)^2 + m_{\Delta_0}^2 \Gamma_\Delta^2}, \quad (8)$$

where  $m_{\Delta_0}$  is the centroid of the resonance,  $\Gamma_\Delta$  is the width of the resonance and  $p_f$  is the center of mass momentum in the  $N\Delta$  channel.

As for the reaction cross section of the reverse reaction, Danielewicz and Bertsch first deduced and obtained the isospin-averaged cross section in the Ref.[39]:

$$\sigma_{N\Delta \rightarrow NN} = \left( \frac{m_\Delta p_f^2 \sigma_{NN \rightarrow N\Delta}}{2(1+\delta)p_i} \right) \times \left( \int_{m_\pi + m_N}^{\sqrt{s} - m_N} \frac{dm_\Delta}{2\pi} P(m_\Delta) \right)^{-1}, \quad (9)$$

where  $p_f$  and  $p_i$  are the nucleon center of mass momenta in the  $NN$  and  $N\Delta$  channels, respectively. The width of  $\Delta$  resonance is given by:

$$\Gamma_\Delta = \frac{0.47q^3}{m_\pi^2 \left[ 1 + 0.6 (q/m_\pi)^2 \right]}, \quad (10)$$

where  $q = \sqrt{\left( \frac{m_\Delta^2 - m_n^2 + m_\pi^2}{2m_\Delta} \right)^2 - m_\pi^2}$ , and  $q$  is the pion momentum in the  $\Delta$  rest frame. For the reaction  $\Delta \rightarrow \pi + N$ , the classical formula  $P_{\text{decay}} = 1 - \exp(-d t \Gamma_\Delta/\hbar)$  is used for the decay probability of the  $\Delta$  particle. As before, a Breit-Wigner function is assumed for the  $\pi + N$  cross section in the reverse reaction [38, 39]:

$$\sigma_{\pi+N} = \sigma_{\text{max}} \left( \frac{q_0}{q} \right)^2 \frac{\frac{1}{4}\Gamma_\Delta^2}{(m_\Delta - m_{\Delta_0})^2 + \frac{1}{4}\Gamma_\Delta^2}, \quad (11)$$

where  $q_0$  is the pion momentum at the centroid of the resonance  $m_{\Delta_0} = 1.232$  GeV.

The maximal cross section  $\sigma_{\text{max}}$  reads as follows:

$$\begin{aligned} \sigma_{\text{max}}^{\pi^+ p \rightarrow \Delta^{++}} &= \sigma_{\text{max}}^{\pi^- n \rightarrow \Delta^-} = 200 \text{mb} \\ \sigma_{\text{max}}^{\pi^- p \rightarrow \Delta^0} &= \sigma_{\text{max}}^{\pi^+ n \rightarrow \Delta^+} = 66.67 \text{mb}. \\ \sigma_{\text{max}}^{\pi^0 p \rightarrow \Delta^+} &= \sigma_{\text{max}}^{\pi^0 n \rightarrow \Delta^0} = 133.33 \text{mb} \end{aligned} \quad (12)$$

All elastic scattering and decay reactions are assumed to be isotropic in this model. Elastic scattering cross sections bear an angular distribution as[40]:

$$\frac{d\sigma_{\text{el}}}{d\Omega} \propto e^{bt}, \quad (13)$$

where  $b = \frac{6[3.65(\sqrt{s} - 1.8766)]^6}{1+[3.65(\sqrt{s} - 1.8766)]^6}$  and  $t = -2p^2(1 - \cos\theta)$ .  $p$  is the momentum of one particle in the center of mass.

Baryon-baryon collisions in the IBUU model are simulated by a Monte Carlo-based modelling process [1]. During a small time interval ( $\delta t = 0.5$  fm/c), one firstly

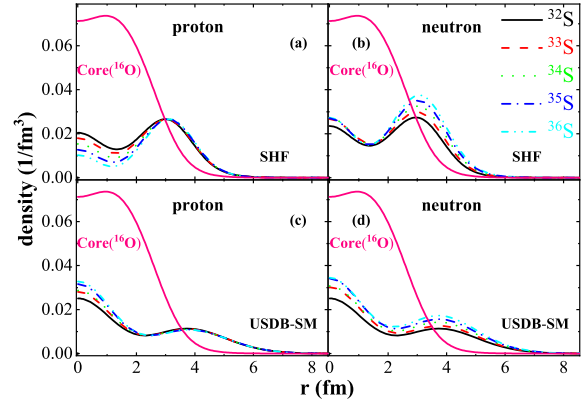


FIG. 1. (Color online) Density distributions of valence protons of sulfur isotopes obtained with SHF (a) and USDB-SM (c), and density distributions of valence neutrons of the same isotopes obtained with SHF (b) and USDB-SM (d). The normalization condition  $4\pi \int_0^{r_{\text{max}}} \rho(r) r^2 dr = A_{\text{val}}$  is used, with  $A_{\text{val}}$  the number of valence nucleons above the  $^{16}\text{O}$  core. The density distributions of protons (a)(c) and neutrons (b)(d) of the  $^{16}\text{O}$  core are also shown in the context of SHF, using the normalization condition  $4\pi \int_0^{r_{\text{max}}} \rho(r) r^2 dr = A_{\text{core}}$ , where  $A_{\text{core}} = 16$ .

checks if two baryons are sufficiently close to interact with each other ( $b_{\text{max}} = \sqrt{\sigma_{\text{nn}}^t(\sqrt{s})/\pi}$ ). If it is the case, one performs simulations to determine which kind of reaction should occur [1]. When scattering occurs between two nucleons, both elastic and inelastic scattering can occur. NN elastic reactions occur with the probability of collision  $P_{\text{elastic}}(NN) = \sigma_{\text{elastic}}/\sigma_{\text{nn}}^t(\sqrt{s})$ .  $P_{\text{inelastic}}(NN \rightarrow N\Delta) = \sigma_{\text{inelastic}}/\sigma_{\text{nn}}^t(\sqrt{s})$  determines the probability of baryon pair formation in the  $NN \rightarrow N\Delta$  reaction, with  $\sigma_{\text{nn}}^t(\sqrt{s})$  the total cross section in the center-of-mass energy  $\sqrt{s}$ , and  $P_{\text{elastic}}(NN) + P_{\text{inelastic}}(NN \rightarrow N\Delta) = 1$ . For the baryon  $\Delta$ , the same treatment has been done in the simulation, which has three branches: i. elastic scattering with the nucleon( $N\Delta$ ); ii. inelastic scattering with the nucleon to produce two nucleons ( $N\Delta \rightarrow NN$ ); iii. decaying to a  $\pi$  meson and a nucleon( $\Delta \rightarrow N\pi$ ). Additionally, the  $\pi$  mesons are absorbed by the nucleons to re-produce baryons.

The present results have been obtained using the IBUU04 program[1, 4, 8–10, 12, 14], using as inputs the nucleon densities calculated with SHF and SM, respectively.  $\pi$  yields are then determined from the Monte Carlo process described above and coded in the IBUU04 program.

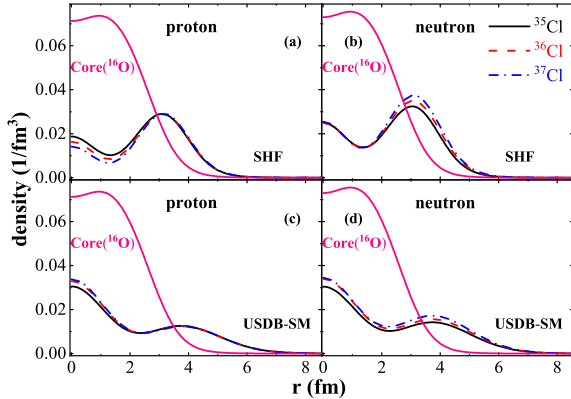


FIG. 2. (Color online) Same as Fig.(1), but for chlorine isotopes.

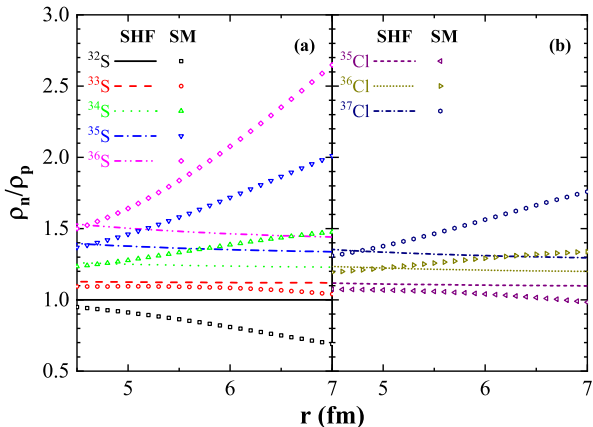


FIG. 3. (Color online) Ratio of neutron density to proton density as a function of radius in the sulfur (a) and chlorine isotopic chain (b), using the USDB-SM and SHF approaches.

### III. NUCLEON DENSITIES IN THE SHF AND USDB-SM APPROACHES

The valence nucleon density distributions of the two colliding nuclei used in the IBUU model (see Eq.(2)) are isotropic. Consequently, only radial densities is needed to be calculated from the SHF and USDB-SM approaches. All nucleons are active in the SHF model. Therefore, approximations are needed to evaluate a function equivalent to the USDB-SM valence nucleon density distribution in a mean-field approach. For this, one firstly calculates the total density of  ${}^A\text{S}$  ( $A = 32 - 36$ ),  ${}^A\text{Cl}$  ( $A = 35 - 37$ ) and  ${}^{16}\text{O}$  with SHF. Valence nucleon distributions in a SHF approach are then defined by subtracting of the density distribution of  ${}^{16}\text{O}$  from the total density distribution of the considered nucleus:

$$\rho_r^{(n,p)}({}^A\text{X(v.n.)}) = \rho_r^{(n,p)}({}^A\text{X}) - \rho_r^{(n,p)}({}^{16}\text{O}) \quad (14)$$

where  $\text{X}=(\text{S},\text{Cl})$  and (v.n.) signifies valence nucleons.

The harmonic oscillator length used in USDB-SM is set to  $b = 1/\alpha = \sqrt{\hbar/\mu\omega_0} = 2.5$  fm. Even though this value of  $b$  is large for the considered region of the nuclear chart, it is for this value that the distributions issued from USDB-SM and SHF have closest maxima, so that it physically sound to use  $b = 2.5$  fm for our purpose. As can be seen from Fig.1 and Fig.2, the calculated density distributions are generated by almost fully by valence nucleons for radii larger than 4.5 fm. In the present paper, we shall consider the reactions of interest have a large impact parameter, equal to  $b_0 = 9$  fm, one can assume that collisions will dominantly involve valence nucleons. The  ${}^{16}\text{O}$  core is then not expected to play a significant role in pion production.

We will consider the following nuclear states:  ${}^{32}\text{S}(0^+)$ ,  ${}^{33}\text{S}(3/2^+)$ ,  ${}^{34}\text{S}(0^+)$ ,  ${}^{35}\text{S}(3/2^+)$ ,  ${}^{36}\text{S}(0^+)$ ,  ${}^{35}\text{Cl}(3/2^+)$ ,  ${}^{36}\text{Cl}(2^+)$  and  ${}^{37}\text{Cl}(3/2^+)$ . The effect of nucleon-nucleon correlations is already seen in Fig.1 and Fig.2, where the extension of USDB-SM density distributions is larger than those arising from SHF. The SHF density distributions have more pronounced local maxima and minima. Moreover, as can be seen in Fig.3, The ratios of the neutron density to proton density in SHF and USDB-SM are close within 5 fm. The change of the ratios is typically faster for radii in USDB-SM than in SHF beyond 5 fm.

### IV. RESULTS AND DISCUSSIONS

In order to distinguish the different inter-nucleon correlations from different structural models, the peripheral nature of valence nucleons distributions is emphasized to avoid the impact of the core.  $\pi$  mesons are expected to be used as probes to explore peripheral properties. The inelastic processes, giving rise to pion production, play a significant role only at beam energies close to 800 MeV/nucleon[16]. Therefore we need the higher energy to produce more mesons to amplify the effect in HIC. we can take a large impact parameter (9 fm) and a high incident beam energy (1 GeV/u). As already mentioned before, the most important region for this type of reaction is the tail of valence-nucleon density distributions. The different asymptotic behaviours of proton and neutron distributions may also play a significant role. The calculated yields of  $\pi^-$ ,  $\pi^+$  are depicted on Fig.4 as functions of momentum with different initializations of valence nucleons profiles in the SHF and USDB-SM approaches for  ${}^A\text{S} + {}^A\text{S}$  and  ${}^A\text{Cl} + {}^A\text{Cl}$  reactions. A large difference in  $\pi^-$  and  $\pi^+$  yields emerges in the results, which is induced by the different nucleon density distributions arising from USDB-SM and SHF. The produced  $\pi$  meson yields are much larger with USDB-SM and are almost twice as large as those provided by SHF under the same entrance channel conditions. The valence nucleon density of USDB-SM is also more important than that of SHF when radii are larger than 4.5 fm. Moreover, the yields of  $\pi^-$ ,  $\pi^+$  share

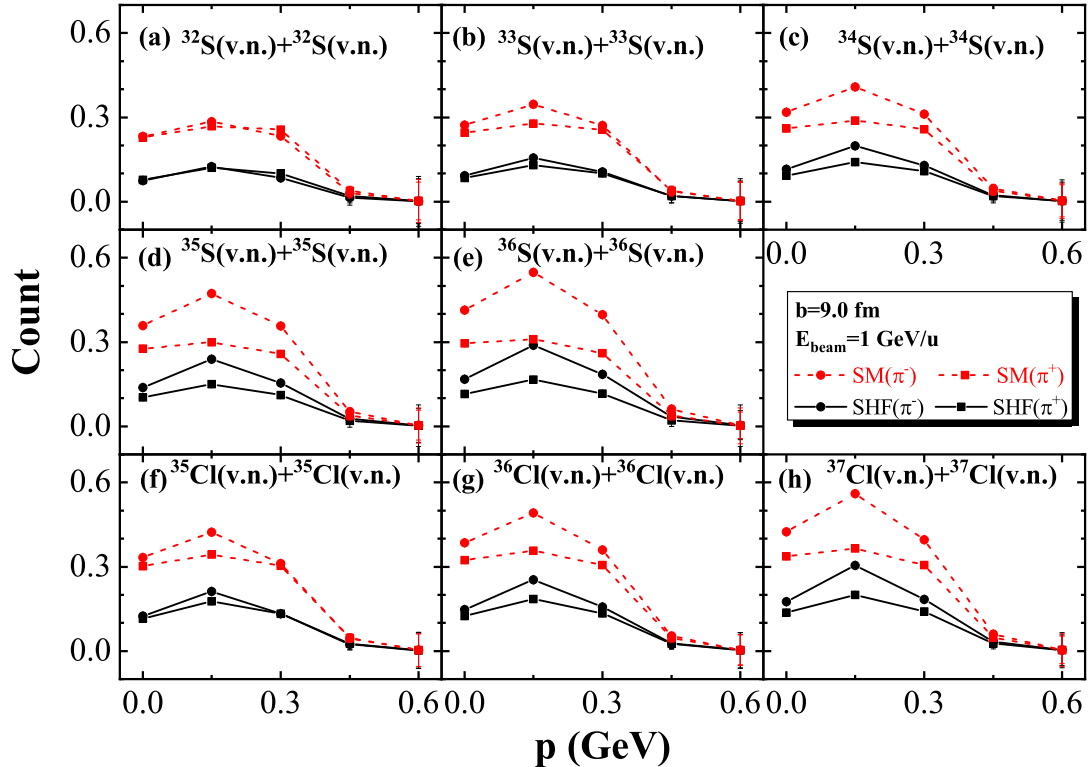


FIG. 4. (Color online) Yields of  $\pi^-$  and  $\pi^+$  mesons as a function of momentum using different density distributions of valence nucleons in SHF and USDB-SM in the  ${}^A\text{S} + {}^A\text{S}$  and in the  ${}^A\text{Cl} + {}^A\text{Cl}$  reactions. One considers sulfur isotopes with  $A = 32$  (a),  $A = 33$  (b),  $A = 34$  (c),  $A = 35$  (d) and  $A = 36$  (e) nucleons in the  ${}^A\text{S} + {}^A\text{S}$  reaction. For the  ${}^A\text{Cl} + {}^A\text{Cl}$  reaction, one considers chlorine isotopes with  $A = 35$  (f),  $A = 36$  (g) and  $A = 37$  (h). The used impact parameter and incident beam energy are 9 fm and 1 GeV/u, respectively.

a common peak at  $p=0.15$  GeV, where the largest differences between SHF and USDB-SM results occur as well. For reaction systems of both sulphur and chlorine isotopes, the yields of  $\pi^-$  mesons increase with the number of neutrons, whereas the yields of  $\pi^+$  mesons are almost constant. This arises because the  $\pi^-$  mesons are mostly produced from neutron-neutron collisions, whereas the  $\pi^+$  mesons are dominantly generated by proton-proton collisions.

The yields of  $\pi^-$ ,  $\pi^+$  are now analyzed as a function of the total number of nucleons  $A$  in the  ${}^A\text{S} + {}^A\text{S}$  and  ${}^A\text{Cl} + {}^A\text{Cl}$  reactions using the different density distributions of valence nucleons in SHF and USDB-SM (see Fig.5). The number of protons does not change in these nuclei, so that the yield of  $\pi^+$  mildly augments. Meanwhile, that of  $\pi^-$  increases rapidly with the number of neutrons. Comparing Fig.5(a) with Fig.5(b), one can see that the S+S and Cl+Cl colliding systems with the same neutron numbers (i.e.,  ${}^{34}\text{S} + {}^{34}\text{S}$  and  ${}^{35}\text{Cl} + {}^{35}\text{Cl}$ ,  ${}^{35}\text{S} + {}^{35}\text{S}$  and  ${}^{36}\text{Cl} + {}^{36}\text{Cl}$ ,  ${}^{36}\text{S} + {}^{36}\text{S}$  and  ${}^{37}\text{Cl} + {}^{37}\text{Cl}$ ) produce nearly the same amount of  $\pi^-$  mesons, but different

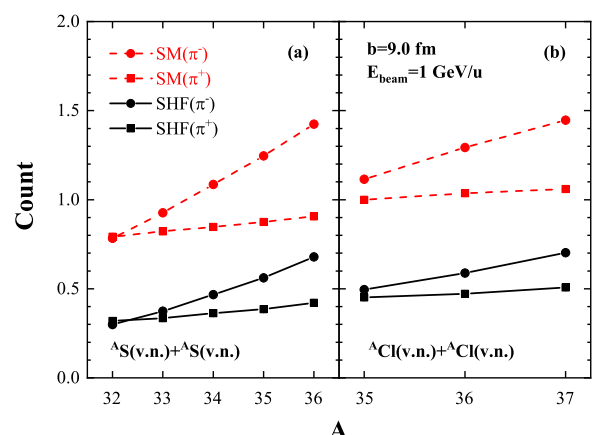


FIG. 5. (Color online) The yields of  $\pi^-$ ,  $\pi^+$  as a function of the number of nucleons  $A$  with different nucleon density distribution in the SHF and USDB-SM model. in the reactions of  ${}^A\text{S} + {}^A\text{S}$  (a) and  ${}^A\text{Cl} + {}^A\text{Cl}$  (b) at an incident beam energy of 1 GeV/nucleon .

amounts of  $\pi^+$  mesons, due to their constant number of neutrons and changing number of protons. Moreover, the yield of  $\pi^+$  mildly augments is due to the fact that about 16% of the  $\pi^+$  mesons are produced from neutron-proton collisions[15].

We now consider the ratio of  $\pi^-/\pi^+$  in the reactions considered above (see Fig.6). The  $\pi^-/\pi^+$  ratio increases with mass number of reaction systems, because the number of protons remains the same while the number of neutrons increases. Consequently, more  $\pi^-$  mesons are produced in a heavier system, so that the  $\pi^-/\pi^+$  ratio augments.

Moreover, the USDB-SM results generate a almost equal slope for the  $\pi^-/\pi^+$  ratio as a function of momentum with those provided by the SHF model. It's due to the  $\rho_n/\rho_p$  ratios in SHF and USDB-SM are close within 5 fm. The  $\rho_n/\rho_p$  ratios above 5 fm have large differences in Fig.3, but there are fewer nuclei here. Thus the density ratio distribution within 5 fm dominates the reaction results, which cause the  $\pi^-/\pi^+$  ratio is not a sensitive observables for the current impact parameters. If larger impact parameters are taken into account, or if a nucleus with larger proton-neutron asymmetry is considered, it is expected that this difference may become larger. The  $\pi^-/\pi^+$  ratio might be a proper observable to distinguish between USDB-SM and SHF in the latter cases. This is worth exploring from an experimental point of view.

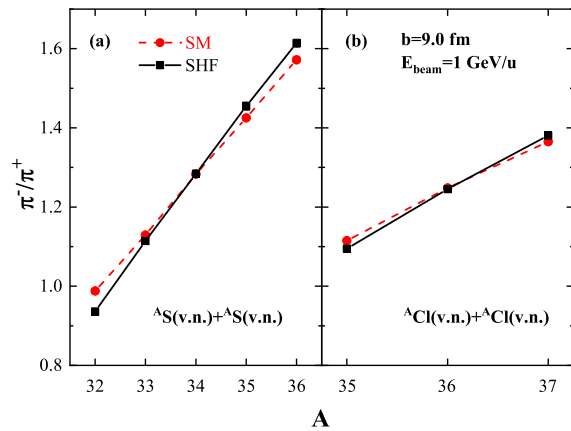


FIG. 6. (Color online)  $\pi^-/\pi^+$  ratio as a function of the number of nucleons  $A$  with different density distributions of valence nucleons in SHF and USDB-SM for the reactions  ${}^A S + {}^A S$  (a) and  ${}^A Cl + {}^A Cl$  (b) reactions at an incident beam energy of 1 GeV/u.

## V. SUMMARY

Pion productions in HIC are depending on the nucleons density distribution of the colliding nuclei during heavy ion collisions. Nucleon densities are typically generated in a mean-field framework. However, inter-nucleon correlations may play an important role in nucleon distribution in nuclei. We have assessed the effect of valence nucleon densities of the initial colliding nuclei in SHF and USDB-SM approaches on pion yields in this work. The USDB-SM allows to include inter-nucleon correlations, which are usually neglected in pion production theoretical calculations.

We considered colliding system of sulfur and chlorine isotopes ( ${}^A S + {}^A S$ ,  ${}^A Cl + {}^A Cl$ ) in our applications pertaining to peripheral collisions. We noticed that pion yields are twice as large when considering inter-nucleon correlations, because densities are enhanced in the surface region, and this augmentation acts similarly on  $\pi^+$  and  $\pi^-$  meson productions. However, the  $\pi^-/\pi^+$  ratio is almost independent of the structure model used in the adopted impact parameter where the  $\rho_n/\rho_p$  ratios of the reacting nucleons in different models are comparable, which is worthy of further study. The noticed increase in  $\pi^+$  and  $\pi^-$  meson yields was seen to be similar using sulfur and chlorine isotopes.

We believe that having experimental pion yields analysed would provide with a completely interesting perspective on the study of the effect of valence nucleon densities in HIC. One could obtain information about the inter-nucleon correlations induced by the nuclear force, which is neglected when using Thomas-Fermi or SHF nucleon densities. Large differences have been noticed to occur in pion yields when nucleon densities are taken from either SHF or USDB-SM calculations. Thus, we suggest that further experimental and theoretical studies should be made to confirm or infirm the dependence of inter-nucleon correlations on the pion production process occurring in heavy ion collisions.

## VI. ACKNOWLEDGEMENTS

Prof. Gao-Chan Yong is greatly thanked for his advice. This work is supported in part by the National Natural Science Foundation of China under Grant Nos. 11775275, 11435014.

---

[1] G. F. Bertsch, S. Das Gupta, Phys. Rep. **160**, 189(1988)  
[2] R. Stock, Phys. Rep. **135**, 259(1986).  
[3] H. Stocker, W. Greiner, Phys. Rep. **137**, 277(1986).  
[4] X. H. Fan, G. C. Yong, W. Zuo, Phys. Rev. C **99**, 041601(R) (2019).  
[5] B. A. Li, Phys. Rev. C **61**, 021903 (2000)  
[6] P. Russotto *et al.*, Phys. Rev. C **94**, 034608 (2016)  
[7] SYMMETRY ENERGY project, <https://groups.nscl.msu.edu/hira/sepweb/pages/home.html>  
[8] Y. F. Guo, G. C. Yong, Phys. Rev. C **100**, 014617 (2019)  
[9] G. C. Yong, Y. Gao, G. F. Wei, Y. F. Guo, W. Zuo, Nucl. Part. Phys. **46** 105105 (2019)

- [10] S. J. Cheng, G. C. Yong, D. H. Wen, Phys. Rev. C **94**, 064621 (2016)
- [11] B. A. Li, C. B. Das, S. D. Gupta, and C. Gale, Phys. Rev. C **69**, 011603(R)(2004)
- [12] Z. X. Yang, X. H. Fan, G. C. Yong, W. Zuo, Phys. Rev. C **98**, 014623 (2018)
- [13] J. Xu, Phys. Rev. C **84**, 064603 (2011)
- [14] G. C. Yong, Phys. Rev. C **96**, 044605 (2017)
- [15] B. A. Li, Phys. Rev. C **71**, 014608 (2005)
- [16] J. R. Stone, P. Danielewicz, Y. Iwata, Phys. Rev. C **96**, 014612(2017)
- [17] G. C. Yong, Eur. Phys. J. A, **52**, 118 (2016)
- [18] T. H. R. Skyrme, Phil. Mag. **1**, 1043 (1956).
- [19] D. Vautherin, D. M. Brink, Phys. Rev. C **5**, 626 (1972).
- [20] M. Grasso, Prog. Part. Nucl. Phys. **106**, 256 (2019).
- [21] T. H. R. Skyrme, Nucl. Phys. **9**, 615 (1959).
- [22] E. Caurier, G. Martínez-Pinedo, F. Nowacki, A. Poves, A. P. Zuker, Rev. Mod. Phys. **77**, 427 (2005).
- [23] Abgrall, Y. G. Baron, E. Caurier, and G. Monsonego, Phys. Lett. B **26**, 53(1967).
- [24] O. Haxel, J. H. D. Jensen, H. E. Suess, Phys. Rev. **75**, 1766 (1949)
- [25] M. Goppert-Mayer, Phys. Rev. **75**, 1969 (1949).
- [26] T. Naito, X. Roca-Maza, G. Colò, H. Z. Liang, Phys. Rev. C **99**, 024309 (2019)
- [27] Y. Zhang, Y. Chen, J. Meng, P. Ring, Phys. Rev. C **95**, 014316 (2017)
- [28] C. A. Bertulani, J. Valencia, Phys. Rev. C **100**, 015802 (2019)
- [29] N. Ullah, Pramana **43** No.2, 165-168(1994)
- [30] D. R. Yennie, D. G. Ravenhall, R. N. Wilson, Phys. Rev. **95**, 500 (1954).
- [31] M. A. Preston, Physics of the nucleus (Addison-Wesley, Reading (Mass.), 1962).
- [32] H. Euteneuer, J. Friedrich and N. Voegler, Nucl. Phys. A **298**, 452 (1978).
- [33] Y. Jin, X. R. Zhou, Y. Y. Cheng, H. J. Schulze, arXiv:1910.05884
- [34] J. Bartel, P. Quentin, M. Brack, C. Guet, H. B. Hakansson, Nucl. Phys. A **386**, 79 (1982).
- [35] B. A. Brown, W. A. Richter, Phys. Rev. C, **74**, 034315 (2006).
- [36] G. C. Yong, Phys. Rev. C **93**, 044610 (2016).
- [37] B. J. VerWest, R. A. Arndt, Phys. Rev. C **25**, 1979(1982)
- [38] B. A. Li, A. T. Sustich, B. Zhang, C. M. Ko, Int. J. Mod. Phys. E **10**, 267 (2001).
- [39] P. Danielewicz, G. F. Bertsch, Nucl. Phys. A **533**, 712(1991)
- [40] J. Cugnon, T. Mizutani, J. Vandermeulen, Nucl. Phys. A **352**, 505 (1981).